European Journal of Medicinal Chemistry 45 (2010) 1415–1423

Contents lists available at ScienceDirect

European Journal of Medicinal Chemistry

journal homepage: http://www.elsevier.com/locate/ejmech

Original article

Synthesis and evaluation of novel rutaecarpine derivatives and related alkaloids derivatives as selective acetylcholinesterase inhibitors

Bin Wang [a,b], Yi-Chi Mai [a], Yue Li [a], Jin-Qiang Hou [a], Shi-Liang Huang [a], Tian-Miao Ou [a], Jia-Heng Tan [a], Lin-Kun An [a], Ding Li [a], Lian-Quan Gu [a,*], Zhi-Shu Huang [a,*]

[a] School of Pharmaceutical Sciences, Sun Yat-sen University, Waihuan East Road 132, Guangzhou 510006, People's Republic of China
[b] Department of Chemistry and Life Science, Xiangnan University, Chenzhou, Hunan 423000, People's Republic of China

ARTICLE INFO

Article history:
Received 7 October 2009
Received in revised form
9 December 2009
Accepted 18 December 2009
Available online 4 January 2010

Keywords:
Rutaecarpine derivatives
Acetylcholinesterase inhibitors
Synthesis
Selectivity

ABSTRACT

A series of novel rutaecarpine derivatives and related alkaloid derivatives 3-aminoalkanamido-substituted rutaecarpine **4a–f** and 7,8-dehydrorutaecarpine **5a–c**, and 6-aminoalkanamido-substituted 3-[2-(3-Indolyl)ethyl]-4(**3a**)-quinazolinones **8a–c**, were synthesized and subjected to pharmacological evaluation as acetylcholinesterase (AChE) inhibitors. The synthetic compounds exhibited strong inhibitory activity for AChE and high selectivity for AChE over BuChE. The structure–activity relationships were discussed and their binding conformation and simultaneous interactions mode were further clarified by kinetic characterization and the molecular docking studies.

1. Introduction

Alzheimer's disease (AD) is an age-related chronic, neurodegenerative disorder characterized by progressive memory loss and other cognitive impairments, which are thought to be related to the degeneration of cholinergic neurons in the cerebral cortex and subcortical structures [1]. Although many factors have been implicated in AD, its etiology and pathogenesis remain unclear. The cholinergic hypothesis, which postulates that at least some of the cognitive decline experienced by AD patients results from a deficiency in acetylcholine (ACh) and thus in cholinergic neurotransmission, represents one of the most useful approaches involved in the design of new agents for the treatment of AD [2]. This strategy is based on the development of drugs with an acetylcholinesterase (AChE) inhibition profile in order to rectify the deficiency of cerebral acetylcholine. Meanwhile, reversibility of inhibitors is an important aspect in the design of AChE inhibitors in AD. Actually reversible inhibitors are useful in AD, and irreversible inhibitors would become nerve agents like organophosphorus type inhibitors. Several compounds have been previously synthesized and determined as reversible and selective AChE inhibitors (AChEI) for symptomatic treatment of AD, such as donepezil, galantamine and rivastigmine.

Cholinesterases constitute a family of enzymes that catalyze the hydrolysis of the neurotransmitter acetylcholine into choline and acetic acid. There are two types of cholinesterases including AChE (EC 3.1.1.7) and BuChE (EC 3.1.1.8) in various tissues of body [3]. The main function of AChE is terminating the impulse transmission at cholinergic synapses rapid hydrolysis by AChE into ACh. Recent studies have identified that AChE could also play a key role in accelerating senile amyloid β-peptide (Aβ) plaques deposition [4]. It is likely that AChE interacted with (Aβ) and promoted amyloid fibril formation through a pool of amino acids located in the proximity of peripheral anionic site (PAS) [5].

However, the functions of BuChE are still not clear. There is some evidence to suggest that BuChE activity may be involved in the pathogenesis of Alzheimer's disease [6]. This has led to the hypothesis that the use of nonselective cholinesterase inhibitors inhibit both BuChE and AChE, which may be more beneficial to patients with Alzheimer's disease than the use of selective cholinesterase inhibitors that inhibit AChE alone [7]. However, inhibition of BuChE, highly abundant outside the brain, may contribute to the peripheral side effects of ChE inhibitors [8]. Dose-response curves for tremor (central effect) and salivation (peripheral effect) showed that more selective AChE inhibitor donepezil

Abbreviations: AD, Alzheimer's disease; AChE, acetylcholinesterase; BuChE, butyrylcholinesterases; Aβ, amyloid β-peptide; PAS, peripheral anionic site; DHED, dehydroevodiamine; SAR, structure–activity relationship.

* Corresponding author. Tel.: +86 20 39949056; fax: +86 20 39943056.
E-mail addresses: cesglq@mail.sysu.edu.cn (L.-Q. Gu), ceshzs@mail.sysu.edu.cn (Z.-S. Huang).

0223-5234/$ – see front matter © 2009 Elsevier Masson SAS. All rights reserved.
doi:10.1016/j.ejmech.2009.12.044

possessed a more favorable therapeutic index than tacrine, which could inhibit both of AChE and BuChE inhibitor (Fig. 1) [9]. In clinical treatment of AD, tacrine shows hepatotoxicity, significant drug–drug interactions, and serious side effects, compared with donepezil, rivastigmine, and galantamine [10]. In addition, it was recently reported that BuChE activity was decreased in synapses of AD patients *in vivo* [11]. All these findings indicated that drug development would be better targeted to increasing AChE inhibition and high selectivity for AChE over BuChE.

The design strategy for AChE inhibitors is based on the study of crystallographic structure of AChE. X-ray crystallography of the AChE/inhibitor complexes indicated that AChE has a catalytic site at the bottom of deep narrow gorge and a peripheral anionic site (PAS) at the entrance. Simultaneous binding with the active site and PAS has been suggest to be important in designing powerful and selective AChE inhibitors [12,13].

Rutaecarpine (**Ru**) is a major quinazolinocarboline alkaloid isolated from Evodia rutaecarpaas shown in Fig. 1. It has been reported to possess a wide spectrum of pharmacological activities, such as vasodilation, antithrombosis, and anti-inflammation [14–16]. It has also been recently reported that the rutaecarpine-type alkaloid dehydroevodiamine (DHED) shows strong anti-amnesic activity *in vivo* with an IC_{50} value of 6.3 μM, combined with a moderate AChE inhibition *in vitro* [17,18]. Based on the structural information of AChE and AChE inhibitors, we designed the AChE inhibitors that can interact simultaneously with both the catalytic and peripheral sites (PAS) of AChE. The general structure designed includes two components separated by a spacer group with a suitable length, with the aromatic ring binding with the PAS of AChE and with the side chain terminal amino group interacting with the catalytic site of AChE. Our introduction of a side chain with terminal amino group in the rutaecarpine could greatly improve AChE inhibitory activity and AChE/BuChE selectivity based on our initial docking study.

Based on our above strategy, a series of new 3-aminoalkanamido-substituted rutaecarpine derivatives were designed and synthesized, and their inhibitory activities for AChE and BuChE were tested according to the modified Ellman method [19]. The structure–activity relationships (SARs) were then discussed.

2. Chemistry

The preparation of a series of rutaecarpine derivatives **4a**–**f**, **5a**–**c** and **8a**–**c** was accomplished using the general methods outlined in Scheme 1. The key intermediates 3-amino-rutaecarpine **1** and 6-amino-3-[2-(3-indolyl)ethyl]-4(**3a**)-quinazolinon **6** were prepared according to the Bergman procedure [20], as shown in Schemes 2 and 3.

The intermediate 3-amino-rutaecarpine **1** was synthesized as outlined in Scheme 2. First, the nitro isatoic anhydride was combined with tryptamine in pyridine containing trifluoroacetic anhydride to give **10**. Then cyclization of **10** provided **11** under reflux in acidic conditions (HCl–AcOH) for 30 min. Treatment of the **11** with hydrogen in the presence of 10% Pd/C provided the compound **12**. Elimination of CF_3H was accomplished by treating **12** with alcoholic KOH to afford **1**.

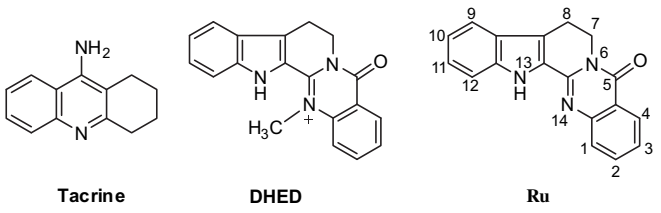

Fig. 1. Structures of donepezil, tacrine, dehydroevodiamine (DHED), rutaecarpine (Ru).

The intermediate 6-amino-3-[2-(3-indolyl)ethyl]-4(**3a**)-quinazolinon **6** was prepared as illustrated in Scheme 3. Treatment of tryptamine with nitro isatoic anhydride in EtOH under reflux gave **13**. Catalytic reduction of **13** with hydrogen in the presence of 10% Pd/C gave the compound **14**. The compound **14** was reacted with refluxing triethyl orthoformate to afford **6**.

The acylation of **1** with the appropriate acid halide gave the haloalkanamide **2a**–**b**. Compound **2a** was treated with DDQ in dioxane to give the haloalkanamide 7,8-dehydrorutaecarpine **3**. However, dehydrogenation of compound **2b** with DDQ in dioxane was failed, therefore the chain elongation was not performed for compounds **5** (**5d**–**f**). Finally, the target compounds **4a**–**f** and **5a**–**c** were obtained by aminolysis of the compounds **2a**–**b** and **3** under reflux by the treatment with the appropriate secondary amines. In addition, 6-amino-alkanamido-substituted 3-[2-(3-indolyl)ethyl]-(**3a**)-quinazolinones derivatives **8a**–**c** were also synthesized following similar procedures.

3. Results and discussion

The inhibitory activity of synthetic derivatives and the original lead compound (**Ru**) was evaluated against AChE and BuChE using tacrine as positive control. The IC_{50} values and selectivity index for the inhibition of AChE and BuChE are summarized in Table 1. All compounds were tested in at least five concentrations covering the range producing less than 20% and greater than 80% inhibition, but limited to 100 μM. Concentration inhibition curves were obtained and their inhibitory concentration (IC_{50}) calculated by nonlinear regression. For comparison, tacrine was tested under the same assay conditions, and gave IC_{50} values of 222.7 nM and 29.98 nM for the inhibition of AChE and BuChE, respectively.

These results showed that all of synthetic derivatives gave higher inhibitory activity against AChE and selectivity for AChE over BuChE comparing with the original lead compound (**Ru**). Compound **5c** was the most potent for AChE inhibition, which presented an IC_{50} value of 10.1 nM. It was indicated that the introduction of the amino-alkanamido-substituted group could significantly increase the inhibitory activity of derivatives. These side chains might be protonated at physiological pH, thus they could occupy the anionic binding site of quaternary amino group via cation–π interaction, and further promote the simultaneous binding interaction of rutaecarpine moieties with PAS of AChE.

After comparing inhibitory activity of synthetic derivatives with different rings (**4a**–**c**, **5a**–**c** and **8a**–**c**), we found that the compounds with aromatic C ring (**5a**–**c**) showed a better activity, which are approximately 5–11-fold stronger than those without aromatic C ring (**4a**–**c**) (Table 1). Derivatives with opened C ring (**8a**–**c**) led to a huge (more than 130-fold compared with **5a**–**c**) decrease in activity, indicating the aromatic planar moiety of compounds could be in favor for interacting to the enzyme-binding site, while the flexibility of molecules might be a disadvantageous factor for binding affinity of compounds with enzyme.

According to the screening data, the structure for terminal groups of side chain also had effects on their inhibitory activities (Table 1). The results were the same as those reported for oxoisoaporphine derivatives by our group [21,22]. The higher inhibitory potency was found to be associated with piperidine at the end of side chain (**4c**, **4f**, **5c**, and **8c**). Diethylamine derivatives (**4a**, **4d**, **5a**, and **8a**) showed less inhibitory activity, which were approximately 3–6-fold lower than corresponding piperidine derivatives. These results indicated that the semi-rigid side chain could be in favor of their entering into the corresponding binding pocket of the

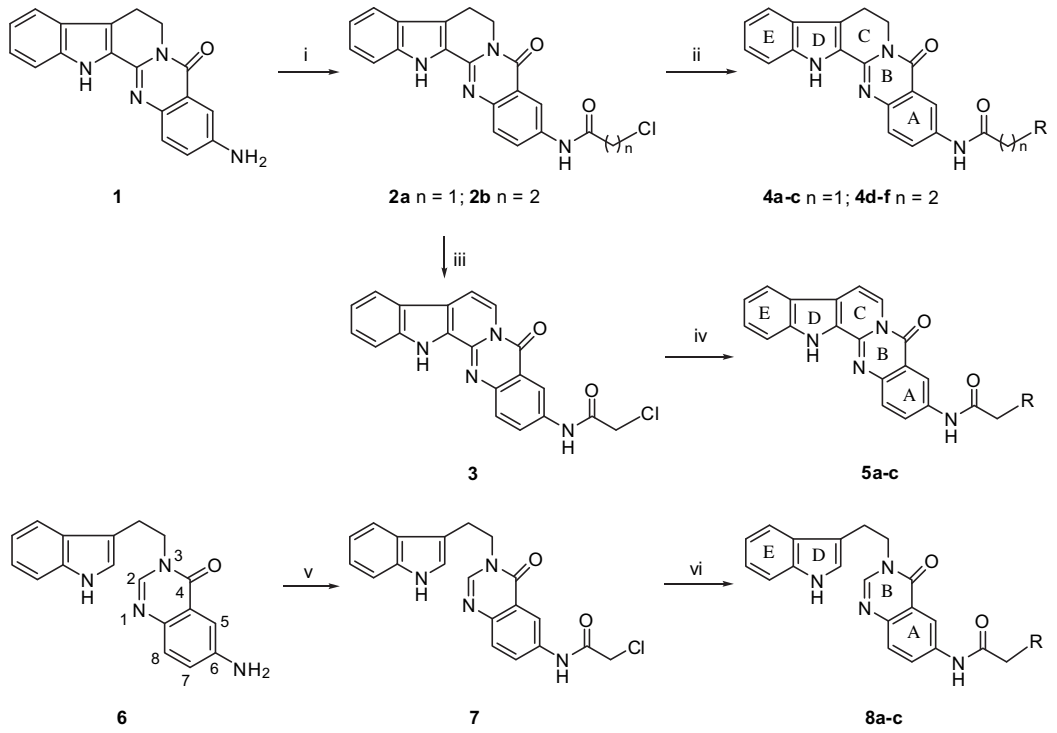

Scheme 1. Synthesis of 3-aminoalkanamido-substituted rutaecarpine and 7,8-dehydro-rutaecarpine, 6-aminoalkanamido-substituted 3-[2-(3-Indolyl)ethyl]-4(**3a**)-quinazolinones derivatives. Reagents and conditions: (i) $ClCO(CH_2)_nCl$, CH_2Cl_2, reflux; (ii) HNR_2, EtOH, KI, reflux; (iii) DDQ, Dioxane, reflux; (iv) HNR_2, EtOH, KI, reflux; (v) $ClCOCH_2Cl$, CH_2Cl_2, reflux; (vi) HNR_2, EtOH, KI, reflux. ('R-' are shown in Table 1).

enzyme. In addition, the elongation of side chain (**4d–f**) significantly increased AChE and BuChE inhibition.

Most of the derivatives were found to be selective for AChE over BuChE. Particularly, Compound **5c** gave the highest inhibitory activity and also the highest selectivity index (539-fold). The derivatives with piperidine at the end of side chain gave more significant selectivity than those with diethylamine or pyrrolidine. Moreover, the selectivity of the derivatives was related with the different backbone and the length of the side chain. The derivatives of the backbone with aromatic C ring (**5a–c**) showed better selectivity than non-aromatic C ring (**4a–c**), while the derivatives of backbone with opened C ring (**8a–c**) were less selective.

The AChE inhibition caused by the most potent compound **5c** was investigated for its time-independence and dialysis after incubation (Fig. 2). For compound **5c** the AChE activity was monitored during incubation with **5c**. It was found that the inhibition was not time-dependent, which exhibits a typical pattern of reversible inhibition. Furthermore, the reversibility of the inhibition process was supported by dialysis of incubation mixture. After dialysis, AChE activity was almost completely recovered (Fig. 2). These results indicate that the inhibition is reversible.

The nature of AChE inhibition caused by the most potent compound **5c** was investigated by the graphical analysis of steady-state inhibition data (Fig. 3). Reciprocal plots (Lineweaver–Burk plots) describing **5c** inhibition showed both increasing slopes and increasing intercepts with higher inhibitor concentration. The pattern indicated the mixed-type inhibition which was similar to that of tacrine. The result revealed that compound **5c** was able to bind both of the active site and PAS of AChE, which was also in agreement with the results of molecular modeling studies.

To explore the possible binding conformation and interaction mode of the compound with *Tc*AChE (PDB code: 1EVE), a molecular modeling study was performed using the docking program AUTODOCK 4.0 package with PyMOL program as shown in Fig. 4

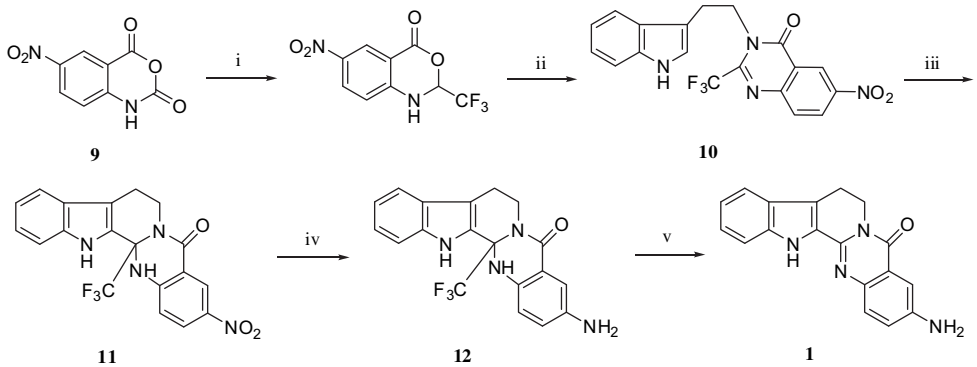

Scheme 2. Synthesis of 3-amino-rutaecarpine **1** according to the Bergman procedure [19]. Reagents and conditions: (i) $(CF_3CO)_2O$, pyridine, 25 °C, 30 min; (ii) tryptamine, 115 °C, 3 h; (iii) HCl, AcOH, reflux, 1 h; (iv) 10% Pd/C, H_2, MeOH, 4 h; (v) KOH, H_2O, EtOH, reflux, 30 min.

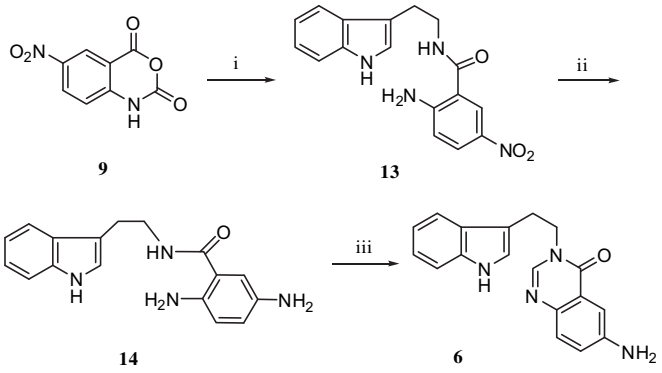

Scheme 3. Synthesis of 6-amino-3-[2-(3-indolyl)ethyl]-4(**3a**)-quinazolinon **6** according to the Bergman procedure [19]. Reagents and conditions: (i) tryptamine, EtOH, reflux, 1 h; (ii) 10% Pd/C, H_2, MeOH, 3 h; (iii) triethyl orthoformate, reflux, 6 h.

[23,24]. The most probable conformation of the ligand **5c** was chosen based on the docked energy value (Fig. 5). The docking result demonstrated that the aromatic A ring in **5c** could stack against PAS residue Phe331 with the ring-to-ring distance being 4.1 Å, as shown in Fig. 3A. The conformation of the side chain made good fit with the shape of the gorge, in the bottom of the gorge, the charged nitrogen of piperidine made a cation–π interaction with the Trp84 and the distance was 4.0 Å. The simultaneous interactions of **5c** in the peripheral pocket and catalytic triad side of *Tc*AChE explained the higher inhibitory potency of AChE, however, different interaction mode were found in **5c** in complex with *Hu*BuChE (PDB code: 1POI), E ring in **5c** could make π–π stacking with the Trp82 in catalytic triade side and the distance was 4.5 Å. Besides this, no other obvious interactions were observed between **5c** and *Hu*BuChE, (Fig. 5). As a result, the compound gave weaker inhibitory activity for BuChE and exhibited higher selectivity for AChE/BuChE. The interaction mode of other derivatives with AChE and BuChE was similar to **5c**. The calculated binding free energy of derivatives in molecular docking was found to correlate well with inhibition, as shown in Table 2.

4. Conclusion

3-Aminoalkanamido-substituted rutaecarpine (**4a–f**) and 7,8-dehydro-rutaecarpine (**5a–c**), as well as 6-aminoalkanamido-substituted 3-[2-(3-indolyl)ethyl]-4(**3a**)-quinazolinones (**8a–c**) derivatives were synthesized and subjected to pharmacological evaluation. The results showed that the synthetic compounds possessed high AChE inhibitory potency. The 3-aminoalkanamido-substituted 7,8-dehydrorutaecarpine derivatives (**5a–c**) showed higher inhibitory effects on AChE. The compounds with piperidine at the end of side chain possessed higher inhibitory activity. In addition, the elongation of side chain significantly increased AChE and BuChE inhibition. Moreover, our synthetic compounds also showed high selectivity for AChE over BuChE. The molecular docking, reversibility and kinetic analysis revealed that the simultaneous interactions in the central pocket, gorge, and peripheral pocket of *Tc*AChE may explain the high reversible inhibitory potency of AChE. Finally, our results indicate that these new compounds represent useful templates for the development of new anti-AD agents.

5. Experimental section

5.1. Chemistry

^{1}H and ^{13}C NMR spectra were recorded using TMS as the internal standard in DMSO-d_6 or $CDCl_3$ with a Bruker BioSpin GmbH spectrometer at 400.132 MHz and 100.614 MHz, respectively; MS spectra were recorded on a Shimadzu LCMS-2010A instrument with an ESI or ACPI mass selective detector. Melting points (mp) were determined using an SRS-*OptiMelt* automated melting point instrument without correction. Elemental analysis was carried out on an Elementar Vario EL CHNS Elemental Analyzer.

6-Nitro-1H-benzo[d][1,3]oxazine-2,4-dione **9** was prepared according to a literature procedure [25].

Table 1
In vitro inhibition IC_{50} and selectivity index of derivatives **4a–f**, **5a–c**, and **8a–c** on AChE and BuChE.

Compound	R	*n*	AChE inhibition[a], nM	BuChE inhibition[b], nM	Selectivity Index[c]
Ru			>100,000	>100,000	–
4a	$-N(CH_2CH_3)_2$	1	372.3 ± 0.9	17,620 ± 150	47.4
4b		1	131.2 ± 0.8	696.1 ± 1.1	5.3
4c		1	111.4 ± 0.9	33,020 ± 90	297.5
4d	$-N(CH_2CH_3)_2$	2	80.20 ± 0.93	2848 ± 6	35.5
4e		2	29.24 ± 0.44	844.5 ± 1.8	28.9
4f		2	21.40 ± 0.05	2112 ± 2	98.7
5a	$-N(CH_2CH_3)_2$	1	57.09 ± 0.68	11,360 ± 64	198.9
5b		1	23.56 ± 0.13	428.2 ± 0.5	18.2
5c		1	10.07 ± 0.32	5429 ± 38	539.1
8a	$-N(CH_2CH_3)_2$	1	7676 ± 44	41,620 ± 140	5.4
8b		1	4044 ± 94	25,860 ± 370	6.4
8c		1	1520 ± 24	12,950 ± 220	8.5
Tacrine			222.7 ± 2.3	29.98 ± 0.27	0.1

[a] 50% inhibitory concentration (means ± SEM of at least four independent experiments) of AChE from *electric eel*.
[b] 50% inhibitory concentration (means ± SEM of at least four independent experiments) of BuChE from *equine serum*.
[c] Selectivity Index for AChE = IC_{50} (BuChE)/IC_{50} (AChE).

5.1.1. 3-Amino-rutaecarpine (*1*)

A mixture of 3-amino-1**3b**-(trifluoromethyl)-**13b**,l4-dihydrorutaecarpine **12** (3.2 g) was added to a hot well-stirred solution of KOH (4.0 g) in ethanol (50 mL) and water (15 mL). The reflux was continued for 30 min, whereupon the mixture was cooled, the precipitate was filtered off and was further purified by recrystallization from hot methanol to give the compound **1** as yellow brown solid in 35% yield; m.p. 270–272 °C; ^{1}H NMR (400 MHz, DMSO-d_6): δ 11.72 (s, 1H), 7.61 (d, 1H, J = 7.9), 7.45 (dd, 2H, J = 8.3, 4.2), 7.29 (s, 1H), 7.22 (t, 1H, J = 7.5), 7.08 (dd, 2H, J = 17.5, 9.1), 5.68 (s, 2H), 4.43 (t, 2H, J = 6.6), 3.13 (t, 2H, J = 6.6); HRMS (ESI): calcd for $(M + H)^+$ ($C_{18}H_{14}N_4O$) requires m/z 303.1246, found 303.1237. Anal. Calcd for $C_{18}H_{14}N_4O$: C, 71.51; H, 4.67; N, 18.53. Found: C, 71.37; H, 4.72; N, 18.33.

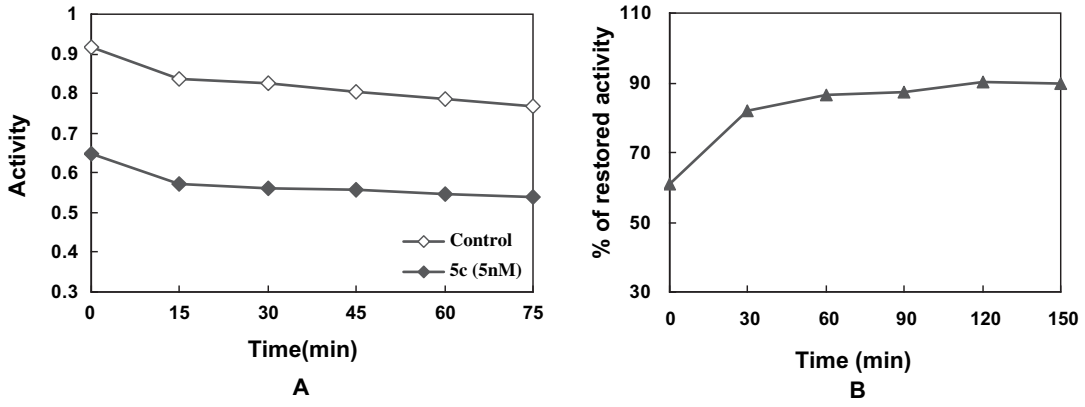

Fig. 2. Reversible inhibition of AChE by **5c**. (A) Time-independence of AChE inhibition; (B) The recovery of AChE activity after dialysis.

*5.1.2. 6-Amino-3-[2-(3-indolyl)ethyl]-4(**3a**)-quinazolinon (**6**)*

A mixture of *N*-(2-(1H-indol-3-yl)ethyl)-2,5-diaminobenzamide **14** (3.2 g) was refluxed with triethyl orthoformate (45 mL) for 6 h, whereupon the clear solution was concentrated to a syrup. The mixture was carefully loaded on a silica gel column and chromatographed using CH_2Cl_2/MeOH (10:1) as eluent to give the compound **6** as pink solid in 31% yield; m.p. 206–207 °C; ^{1}H NMR (400 MHz, DMSO-d_6): δ 11.61 (s, 1H), 9.70 (s, 1H), 7.60 (s, 1H), 7.51 (s, 2H), 7.41 (d, 1H, J = 8.6), 7.26 (s, 1H), 7.24 (s, 1H), 7.05 (s, 1H), 6.85 (t, 1H, J = 7.3), 5.69 (s, 2H), 3.35 (s, 2H), 2.30 (s, 2H); HRMS (ESI): calcd for $(M + H)^+$ ($C_{18}H_{16}N_4O$) requires m/z 305.1402, found 305.1394. Anal. Calcd for $C_{18}H_{16}N_4O$: C, 71.04; H, 5.30; N, 18.41. Found: C, 70.09; H, 5.32; N, 18.46.

5.1.2.1. General acylation procedure. A solution of the appropriate acid halide (4.8 mmol) in CH_2Cl_2 (5 mL) was added during to a well-stirred mixture of the amino-substituted compounds **1** or **6**, (4 mmol) and K_2CO_3 (0.8 g) in CH_2Cl_2 (75 mL) at room temperature. After completed addition the solution was finally refluxed for 4–6 h. After cooling to 0–5 °C, the precipitate formed was filtered off and was further purified by flash column chromatography with petroleum ether/EtOAc (10:1) elution to give the compounds **2a**–**b** or **7**.

*5.1.3. 3-(2-Chloro-acetamino)-rutaecarpine (**2a**)*

The compound **1** was treated with chloroacetyl chloride according to general acylation procedure to afford **2a** as yellow-green solid in 77% yield; m.p. 281–283 °C; ^{1}H NMR (400 MHz, DMSO-d_6): δ 11.86 (s, 1H), 10.67 (s, 1H), 8.49 (d, 1H, J = 2.1), 7.98 (dd, 1H, J = 8.8, 2.3), 7.67 (dd, 2H, J = 16.1, 8.4), 7.48 (d, 1H, J = 8.3), 7.26 (t, 1H, J = 7.7), 7.09 (t, 1H, J = 7.5), 4.46 (t, 2H, J = 6.8), 4.32 (s, 2H), 3.18 (t, 2H, J = 6.8); HRMS (ESI): calcd for $(M + H)^+$ ($C_{20}H_{15}N_4O_2Cl$) requires m/z 379.0962, found 379.0941. Anal. Calcd for $C_{20}H_{15}N_4O_2Cl$: C, 63.41; H, 3.99; N, 14.79. Found: C, 63.28; H, 3.98; N, 14.50.

*5.1.4. 3-(2-Chloro-propionamino)-rutaecarpine (**2b**)*

The compound **1** was treated with 3-chloropropanoyl chloride according to general acylation procedure to afford **2b** as green solid in 70% yield; m.p. 275–277 °C; ^{1}H NMR (400 MHz, DMSO-d_6): δ 11.84 (s, 1H), 10.44 (s, 1H), 8.51 (d, 1H, J = 2.3), 8.00 (dd, 1H, J = 8.8, 2.4), 7.66 (dd, 2H, J = 14.1, 8.4), 7.49 (d, 1H, J = 8.2), 7.26 (t, 1H, J = 7.5), 7.09 (t, 1H, J = 7.4), 4.46 (t, 2H, J = 6.8), 3.93 (t, 2H, J = 6.2), 3.17 (t, 2H, J = 6.8), 2.89 (t, 2H, J = 6.2); HRMS (ESI): calcd for $(M + H)^+$ ($C_{21}H_{17}N_4O_2Cl$) requires m/z 393.1118, found 393.1097. Anal. Calcd for $C_{21}H_{17}N_4O_2Cl$: C, 64.21; H, 4.36; N, 14.26. Found: C, 64.04; H, 4.33; N, 13.98.

*5.1.5. 6-(2-Chloro-acetamino)-3-[2-(3-indolyl)ethyl]-4(**3a**)-quinazolinon (**7**)*

The compound **6** was treated with chloroacetyl chloride according to general acylation procedure to afford **7** as white-pink solid in 67% yield; m.p. 270–272 °C; ^{1}H NMR (400 MHz, DMSO-d_6):

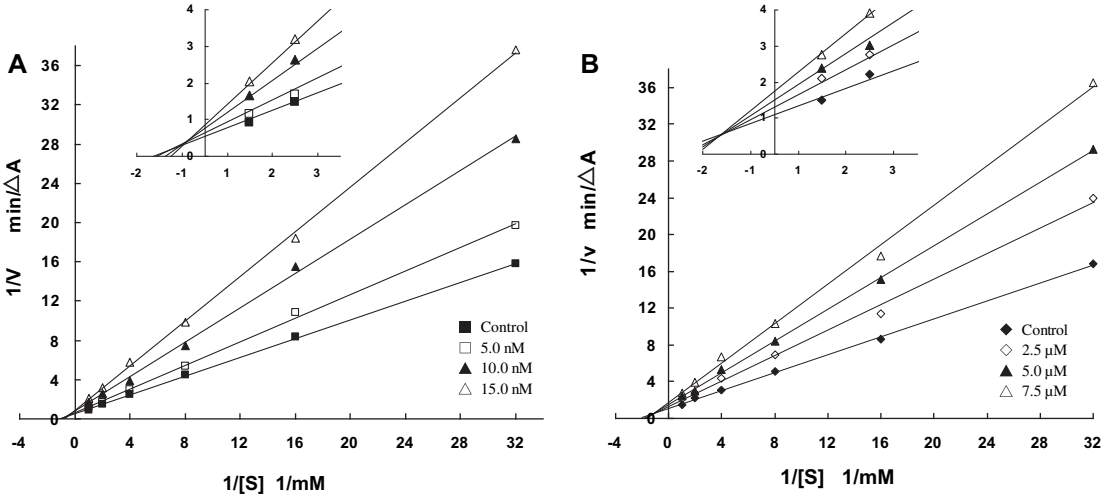

Fig. 3. Lineweaver–Burk plots of the inhibition kinetics of AChE (A) and BuChE (B) by compound **5c**. Inserts were the enlarged plots.

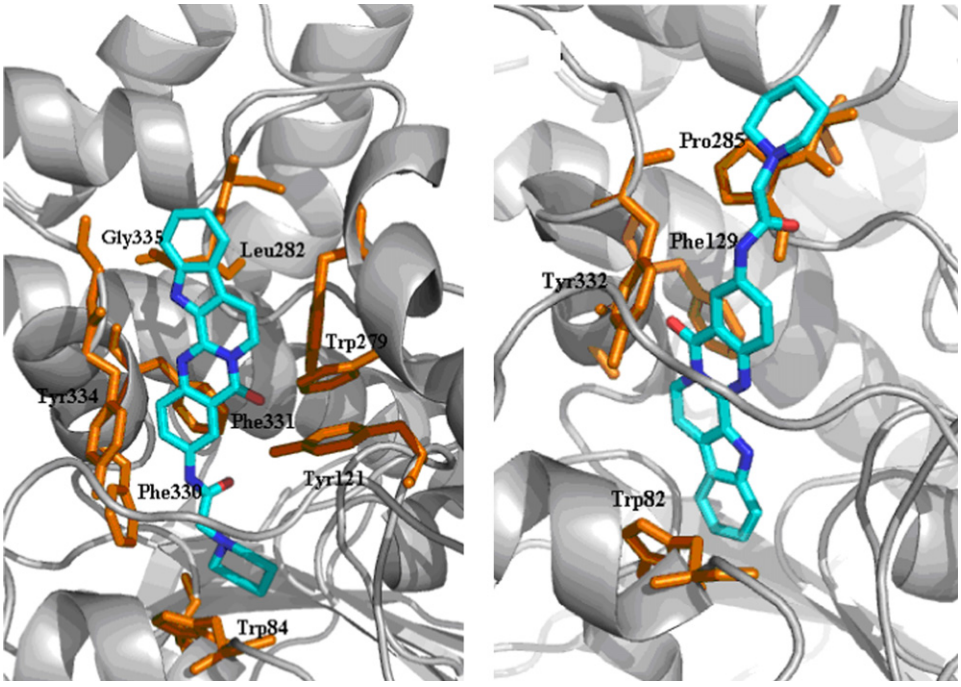

Fig. 4. Docking models of compound–enzyme complex. Representations of compound **5c** interacting with residues in the binding site of *Tc*AChE (left) and *Hu*BuChE (right). The compounds are rendered in blue stick models, and the residues are rendered in golden sticks. Pictures are created with PyMOL [24].

δ 10.84 (s, 1H), 10.72 (s, 1H), 8.53 (s, 1H), 8.00 (d, 1H, $J = 1.9$), 7.96–7.86 (m, 1H), 7.65–7.54 (m, 2H), 7.33 (d, 1H, $J = 8.1$), 7.11 (s, 1H), 7.06 (t, 1H, $J = 7.5$), 6.94 (d, 1H, $J = 14.8$), 4.31 (d, 2H, $J = 1.0$), 4.23 (t, 4H, $J = 7.2$), 3.12 (t, 2H, $J = 7.1$); HRMS (ESI): calcd for $(M + H)^+$ ($C_{20}H_{17}N_4O_2Cl$) requires *m/z* 381.1118, found 381.1094. Anal. Calcd for $C_{20}H_{17}N_4O_2Cl$: C, 63.08; H, 4.50; N, 14.71. Found: C, 63.28; H, 4.52; N, 14.75.

5.1.6. 3-(2-Chloro-acetamino)-7,8-dehydrorutaecarpine (**3**)

A solution of DDQ (0.54 g) in dioxane (10 mL) was added to a hot solution of **2a** (0.76 g) in dioxane (50 mL). After a reflux period 4 h the precipitate formed was filtered and treated with a solution of KOH (1.5 g) in water (25 mL). This procedure was repeated until all DDQ-2H had been removed. The solid obtained was purified by recrystallization from EtOH/DMF (5:1 v/v) to give the compound **3** as brown solid in 26% yield; m.p. 299–301 °C; ^{1}H NMR (400 MHz, DMSO-d_6): δ 12.68 (s, 1H), 10.69 (s, 1H), 8.71 (s, 1H), 8.61 (d, 1H, $J = 7.4$), 8.16 (d, $J = 7.9$, 1H), 8.07 (d, 1H, $J = 8.8$), 7.84 (dd, 2H, $J = 14.0$, 8.3), 7.69 (d, 1H, $J = 8.2$), 7.49 (t, 1H, $J = 7.5$), 7.29 (t, 1H, $J = 7.4$), 4.34 (s, 2H); HRMS (ESI): calcd for $(M + H)^+$ ($C_{20}H_{13}N_4O_2Cl$) requires *m/z* 377.0805, found 377.0763. Anal. Calcd for $C_{20}H_{13}N_4O_2Cl$: C, 63.75; H, 3.48; N, 14.87. Found: C, 63.71; H, 3.64; N, 14.75.

5.1.6.1. General aminolysis procedure. To a stirred refluxing suspension of the haloalkanamido-substituted compounds **2a–b**, **3** or **7** (1.5 mmol) and NaI (0.15 g) in EtOH (40 mL) was added dropwise appropriate secondary amine (1.0 mL) in EtOH (10 mL). The mixture was stirred at reflux for 3 h, cooled to 0 °C, filtered, and washed with ether and water, then evaporated under vacuum. The crude solid was purified by chromatography with petroleum ether/EtOAc (20:1) elution or crystallization from EtOH/DMF (5:1 v/v) to afford **4a–f**, **5a–c** and **8a–c**.

5.1.7. 3-(2-Diethylamino-acetamino)-rutaecarpine (***4a***)

The compound **2a** was treated with excess diethylamine according to general acylation procedure to afford **4a**, after column chromatography with petroleum ether/EtOAc (20:1) elution, as gray solid in 52% yield; m.p. 271–272 °C; ^{1}H NMR (400 MHz, DMSO-d_6): δ 11.83 (s, 1H), 10.02 (s, 1H), 8.54 (d, 1H, $J = 2.4$), 8.06 (dd, 1H, $J = 8.8$, 2.4), 7.65 (dd, 2H, $J = 8.4$, 3.1), 7.49 (d, 1H, $J = 8.3$), 7.26 (t, 1H, $J = 7.6$), 7.09 (t, 1H, $J = 7.4$), 4.46 (t, 2H, $J = 6.8$), 3.19 (dd, 4H, $J = 15.4$, 8.6), 2.63 (q, 4H, $J = 7.1$), 1.04 (t, 6H, $J = 7.1$); HRMS (ESI): calcd for $(M + H)^+$ ($C_{24}H_{25}N_5O_2$) requires *m/z* 416.2087, found 416.2037. Anal. Calcd for $C_{24}H_{25}N_5O_2 \cdot H_2O$: C, 66.49; H, 6.28; N, 16.16. Found: C, 66.28; H, 6.24; N, 16.16.

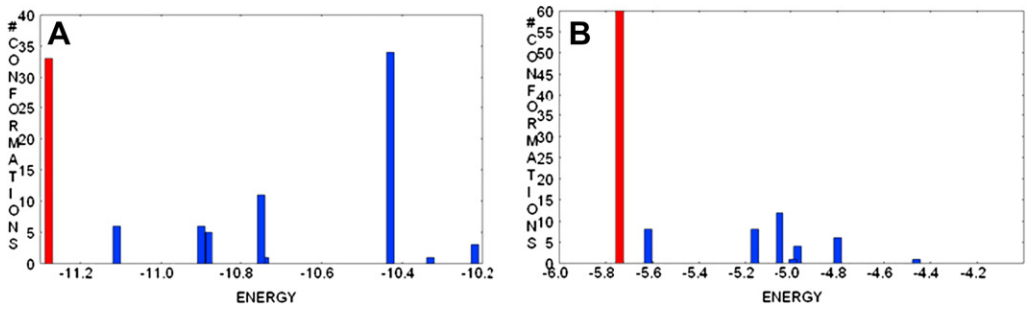

Fig. 5. Clustering analysis of docking conformation of **5c** with AChE (A) and BuChE(B), the red bar are the most probable conformations with the lowest docked energy.

Table 2
The calculated free energies of derivatives in molecular docking.

Compound	Calculated free energy (kcal/mol)/AChE	Calculated free energy (kcal/mol)/BuChE
4c	−10.56	−4.78
4f	−11.06	−6.32
5a	−10.89	−4.91
5b	−11.08	−5.65
5c	−11.28	−5.74
8c	−10.20	−5.38

*5.1.8. 3-(2-N-Pyrrolyl-acetamino)-rutaecarpine (**4b**)*

The compound **2a** was treated with excess pyrrolidine according to general acylation procedure to afford **4b**, after column chromatography with petroleum ether/EtOAc (20:1) elution, as beige solid in 40% yield; m.p. 269–271 °C; ^{1}H NMR (400 MHz, DMSO-d_6): δ 11.84 (s, 1H), 10.10 (s, 1H), 8.55 (d, 1H, J = 2.4), 8.06 (dd, 1H, J = 8.8, 2.5), 7.65 (d, 2H, J = 8.7), 7.48 (d, 1H, J = 8.3), 7.26 (t, 1H, J = 7.5), 7.09 (t, 1H, J = 7.4), 4.46 (t, 2H, J = 6.8), 3.30 (s, 2H), 3.18 (t, 2H, J = 6.8), 2.69–2.53 (m, 4H), 1.76 (dt, 4H, J = 6.2, 3.1); HRMS (ESI): calcd for $(M + H)^+$ ($C_{24}H_{23}N_5O_2$) requires m/z 414.1930, found 414.1867. Anal. Calcd for $C_{24}H_{23}N_5O_2 \cdot H_2O$: C, 66.81; H, 5.84; N, 16.23. Found: C, 66.78; H, 5.51; N, 16.28.

*5.1.9. 3-(2-N-Piperidyl-acetamino)-rutaecarpine (**4c**)*

The compound **2a** was treated with excess piperidine according to general acylation procedure to afford **4c**, after column chromatography with petroleum ether/EtOAc (20:1) elution, as beige solid in 67% yield; m.p. 267–269 °C; ^{1}H NMR (400 MHz, DMSO-d_6): δ 11.85 (s, 1H), 10.07 (s, 1H), 8.53 (d, 1H, J = 2.4), 8.05 (dd, 1H, J = 8.8, 2.4), 7.66 (dd, 2H, J = 8.0, 5.7), 7.48 (d, 1H, J = 8.2), 7.26 (t, 1H, J = 7.5), 7.09 (t, 1H, J = 7.5), 4.46 (t, 2H, J = 6.8), 3.34 (s, 2H), 3.18 (t, 4H, J = 6.8), 3.13 (s, 2H), 1.67–1.48 (m, 4H), 1.42 (d, 2H, J = 4.2); HRMS (ESI): calcd for $(M + H)^+$ ($C_{25}H_{25}N_5O_2$) requires m/z 428.2087, found 428.2052. Anal. Calcd for $C_{25}H_{25}N_5O_2 \cdot H_2O$: C, 67.40; H, 6.11; N, 15.72. Found: C, 67.33; H, 5.98; N, 15.50.

*5.1.10. 3-(2-Diethylamino-propionamino)-rutaecarpine (**4d**)*

The compound **2b** was treated with excess diethylamine according to general acylation procedure to afford **4d**, after column chromatography with petroleum ether/EtOAc (20:1) elution, as white-pink solid in 37% yield; m.p. 315–317 °C; ^{1}H NMR (400 MHz, DMSO-d_6): δ 11.84 (s, 1H), 10.55 (s, 1H), 8.50 (d, 1H, J = 2.2), 8.00 (dd, 1H, J = 8.8, 1.9), 7.64 (dd, 2H, J = 8.1, 5.6), 7.48 (d, 1H, J = 8.2), 7.26 (t, 1H, J = 7.6), 7.09 (t, 1H, J = 7.5), 4.45 (t, 2H, J = 6.7), 3.17 (t, 2,H J = 6.7), 2.77 (t, 2H, J = 6.9), 2.51 (dd, 4H, J = 10.6, 3.6), 2.47 (d, 2H, J = 7.2), 0.99 (t, 6H, J = 7.1); HRMS (ESI): calcd for $(M + H)^+$ ($C_{25}H_{27}N_5O_2$) requires m/z 430.2243, found 430.2210. Anal. Calcd for $C_{25}H_{27}N_5O_2 \cdot H_2O$: C, 67.09; H, 6.53; N, 15.65. Found: C, 67.00; H, 6.44; N, 15.38.

*5.1.11. 3-(2-N-Pyrrolyl-propionamino)-rutaecarpine (**4e**)*

The compound **2b** was treated with excess pyrrolidine according to general acylation procedure to afford **4e**, after column chromatography with petroleum ether/EtOAc (20:1) elution, as beige solid in 28% yield; m.p. 255–256 °C; ^{1}H NMR (400 MHz, DMSO-d_6): δ 11.84 (s, 1H), 10.50 (s, 1H), 8.52 (d, 1H, J = 2.2), 7.99 (dd, 1H, J = 8.8, 2.3), 7.64 (dd, 2H, J = 8.3, 4.9), 7.48 (d, 1H, J = 8.3), 7.26 (t, 1H, J = 7.6), 7.09 (t, 1H, J = 7.5), 4.46 (t, 2H, J = 6.8), 3.17 (t, 2H, J = 6.8), 2.76 (t, 2H, J = 7.0), 2.55 (t, 2H, J = 7.1), 2.51–2.44 (m, 4H), 1.77–1.62 (m, 4H); HRMS (ESI): calcd for $(M + H)^+$ ($C_{25}H_{25}N_5O_2$) requires m/z 428.2087, found 428.2061. Anal. Calcd for $C_{25}H_{25}N_5O_2 \cdot H_2O$: C, 67.40; H, 6.11; N, 15.72. Found: C, 67.21; H, 5.96; N, 15.65.

*5.1.12. 3-(2-N-Piperidyl-propionamino)-rutaecarpine (**4f**)*

The compound **2b** was treated with excess piperidine according to general acylation procedure to afford **4f**, after column chromatography with petroleum ether/EtOAc (20:1) elution, as gray solid in 22% yield; m.p. 260–262 °C; ^{1}H NMR (400 MHz, DMSO-d_6): δ 11.84 (s, 1H), 10.59 (s, 1H), 8.50 (d, 1H, J = 2.2), 7.98 (dd, 1H, J = 8.8, 2.4), 7.65 (dd, 2H, J = 8.2, 6.1), 7.48 (d, 1H, J = 8.3), 7.26 (t, 1H, J = 7.6), 7.09 (t, 1H, J = 7.5), 4.45 (t, 2H, J = 6.8), 3.17 (t, 2H, J = 6.8), 2.63 (d, 2H, J = 6.5), 2.53 (d, 2H, J = 6.7), 2.49–2.29 (m, 4H), 1.57–1.46 (m, 4H), 1.40 (d, 2H, J = 4.8); HRMS (ESI): calcd for $(M + H)^+$ ($C_{26}H_{27}N_5O_2$) requires m/z 442.2243, found 442.2212. Anal. Calcd for $C_{26}H_{27}N_5O_2 \cdot H_2O$: C, 67.95; H, 6.36; N, 15.24. Found: C, 67.68; H, 6.16; N, 15.22.

*5.1.13. 3-(2-Diethylamino-acetamino)-7,8-dehydrorutaecarpine (**5a**)*

The compound **3** was treated with excess diethylamine according to general acylation procedure to afford **5a**, after crystallization from EtOH/DMF (5:1 v/v), as brown solid in 27% yield; m.p. 297–299 °C; ^{1}H NMR (400 MHz, DMSO-d_6): δ 12.71 (s, 1H), 10.12 (s, 1H), 8.77 (d, 1H, J = 10.8), 8.62 (d, 1H, J = 7.4), 8.18 (d, 2H, J = 8.1), 7.85 (t, 2H, J = 10.8), 7.69 (d, 1H, J = 8.1), 7.50 (t, 1H, J = 7.4), 7.30 (t, 1H, J = 7.3), 3.26 (s, 2H), 2.68 (t, 4H, J = 18.0), 1.06 (t, 6H, J = 6.9); HRMS (ESI): calcd for $(M + H)^+$ ($C_{24}H_{23}N_5O_2$) requires m/z 414.1930, found 414.1859. Anal. Calcd for $C_{25}H_{23}N_5O_2 \cdot 2H_2O$: C, 65.06; H, 5.90; N, 15.17. Found: C, 65.03; H, 5.91; N, 15.10.

*5.1.14. 3-(2-N-Pyrrolyl-acetamino)-7,8-dehydrorutaecarpine (**5b**)*

The compound **3** was treated with excess pyrrolidine according to general acylation procedure to afford **5b**, after crystallization from EtOH/DMF (5:1 v/v), as brown solid in 30% yield; m.p. 261–263 °C; ^{1}H NMR (400 MHz, DMSO-d_6): δ 12.70 (s, 1H), 10.20 (s, 1H), 8.78 (s, 1H), 8.62 (d, 1H, J = 7.4), 8.22–8.10 (m, 2H), 7.83 (d, 2H, J = 6.6), 7.69 (d, 1H, J = 8.0), 7.50 (t, 1H, J = 7.2), 7.30 (t, 1H, J = 7.2), 3.34 (s, 2H), 2.75–2.57 (m, 4H), 1.89–1.68 (m, 4H); HRMS (ESI): calcd for $(M + H)^+$ ($C_{24}H_{21}N_5O_2$) requires m/z 412.1774, found 412.1765. Anal. Calcd for $C_{24}H_{21}N_5O_2 \cdot 2H_2O$: C, 64.42; H, 5.63; N, 15.65. Found: C, 64.53; H, 5.64; N, 15.73.

*5.1.15. 3-(2-N-Piperidyl-acetamino)-7,8-dehydrorutaecarpine (**5c**)*

The compound **3** was treated with excess piperidine according to general acylation procedure to afford **5b**, after crystallization from EtOH/DMF (5:1 v/v), as brown solid in 21% yield; m.p. 281–283 °C; ^{1}H NMR (400 MHz, DMSO-d_6): δ 12.71 (s, 1H), 10.16 (s, 1H), 8.77 (s, 2H), 8.62 (d, 1H, J = 7.4), 8.27–8.08 (m, 2H), 7.84 (d, 2H, J = 6.3), 7.68 (d, 1H, J = 8.1), 7.50 (t, 1H, J = 7.4), 7.30 (t, 1H, J = 7.2), 3.16 (s, 2H), 2.49–2.42 (m, 2H), 1.51 (d, 6H, J = 70.1); HRMS (ESI): calcd for $(M + H)^+$ ($C_{25}H_{23}N_5O_2$) requires m/z 426.1930, found 426.1894. Anal. Calcd for $C_{25}H_{23}N_5O_2 \cdot 2H_2O$: C, 65.06; H, 5.90; N, 15.17. Found: C, 65.02; H, 5.93; N, 15.18.

*5.1.16. 6-(2-Diethylamino-acetamino)-3-[2-(3-indolyl)ethyl]-4(**3a**)-quinazolinon (**8a**)*

The compound **7** was treated with excess diethylamine according to general acylation procedure to afford **8a**, after column chromatography with petroleum ether/EtOAc (20:1) elution, as white solid in 67% yield; m.p. 183–185 °C; ^{1}H NMR (400 MHz, DMSO-d_6): δ 10.89 (s, 1H), 10.06 (s, 1H), 8.60 (d, 1H, J = 1.9), 8.03 (d, 1H, J = 2.1), 7.99 (s, 1H), 7.59 (t, 2H, J = 9.4), 7.35 (d, 1H, J = 8.1), 7.12 (d, 1H, J = 2.2), 7.07 (t, 1H, J = 7.5), 6.96 (t, 1H, J = 7.4), 4.25 (t, 2H, J = 7.1), 3.22 (s, 2H), 3.13 (t, 2H, J = 7.1), 2.62 (q, 4H, J = 7.1), 1.04 (t, 6H, J = 7.1); HRMS (ESI): calcd for $(M + H)^+$ ($C_{24}H_{27}N_5O_2$) requires m/z 418.2243, found 418.2231. Anal. Calcd for $C_{24}H_{27}N_5O_2$: C, 69.04; H, 6.52; N, 16.77. Found: C, 68.86; H, 6.35; N, 16.50.

*5.1.17. 6-(2-N-Pyrrolyl-acetamino)-3-[2-(3-Indolyl)ethyl]-4(**3a**)-quinazolinon (**8b**)*

The compound **7** was treated with excess pyrrolidine according to general acylation procedure to afford **8b**, after column chromatography with petroleum ether/EtOAc (20:1) elution, as white-pink solid in 40% yield; m.p. 188–190 °C; ^{1}H NMR (400 MHz, DMSO-d_6): δ 10.86 (s, 1H), 10.11 (s, 1H), 8.59 (d, 1H, J = 2.4), 8.01 (d, 1H, J = 2.5), 7.99 (s, 1H), 7.59 (dd, 2H, J = 11.2, 8.4), 7.34 (d, 1H, J = 8.1), 7.12 (d, 1H, J = 2.2), 7.06 (dd, 1H, J = 11.1, 4.0), 6.99–6.94 (m, 1H), 4.24 (t, 2H, J = 7.2), 3.31 (s, 2H), 3.13 (t, 2H, J = 7.2), 2.62 (t, 4H, J = 5.2), 1.81–1.74 (m, 4H); HRMS (ESI): calcd for $(M + H)^+$ ($C_{24}H_{25}N_5O_2$) requires m/z 416.2087, found 416.2058. Anal. Calcd for $C_{24}H_{25}N_5O_2$: C, 69.38; H, 6.06; N, 16.86. Found: C, 69.19; H, 6.07; N, 16.87.

*5.1.18. 6-(2-N-Piperidyl-acetamino)-3-[2-(3-Indolyl)ethyl]-4(**3a**)-quinazolinon (**8c**)*

The compound **7** was treated with excess piperidine according to general acylation procedure to afford **8b**, after column chromatography with petroleum ether/EtOAc (20:1) elution, as yellow-white solid in 14% yield; m.p. 161–163 °C; ^{1}H NMR (400 MHz, DMSO-d_6): δ 10.86 (s, 1H), 10.05 (s, 1H), 8.58 (d, 1H, J = 2.4), 8.01 (d, 1H, J = 2.5), 7.99 (d, 1H, J = 2.5), 7.59 (t, 2H, J = 8.7), 7.34 (d, 1H, J = 8.1), 7.12 (d, 1H, J = 2.2), 7.10–7.03 (m, 1H), 6.99–6.93 (m, 1H), 4.25 (t, 2H, J = 7.2), 3.30 (s, 2H), 3.15–3.10 (m, 4H), 1.61–1.55 (m, 4H), 1.42 (d, 2H, J = 4.8), 1.20 (d, J = 24.7, 2H); HRMS (ESI): calcd for $(M + H)^+$ ($C_{25}H_{27}N_5O_2$) requires m/z 430.2243, found 430.2214. Anal. Calcd for $C_{25}H_{27}N_5O_2$: C, 69.91; H, 6.34; N, 16.31. Found: C, 70.05; H, 6.58; N, 16.49.

*5.1.19. 3-(2-(1H-Indol-3-yl)ethyl)-6-nitro-2-(trifluoromethyl)-quinazolin-4(3H)-one (**10**)*

To a solution of the 6-Nitro-1H-benzo[d][1,3]oxazine-2,4-dione **9** (5.2 g) in dried pyridine (100 mL) a solution of trifluoroacetic anhydride (3.7 mL) in dried pyridine (4 mL)was dropwise added at room temperature and the stirring was continued for an additional 30 min. After completed addition the solution was finally refluxed for 30 min, whereupon tryptamine (3.2 g) was added and the reflux then continued for 3 h. After cooling the reaction mixture was poured into cold water (500 mL), and the precipitate formed was filtered off, washed with water. The solid obtained was treated with hot methanol to yield yellow crystals (82%). m.p. 244–246 °C; ^{1}H NMR (400 MHz, DMSO-d_6): δ 10.97 (s, 1H), 9.12 (s, 1H), 8.56 (d, 1H, J = 2.7), 8.26 (dd, 1H, J = 9.0, 2.7), 7.59 (dd, 1H, J = 11.4, 8.1), 7.27 (t, 1H, J = 7.1), 7.10 (m, 2H), 3.00 (dd, 2H J = 15.7, 3.1), 2.84 (m, 2H); ESI-MS m/z: 401 $[M - H]^-$.

*5.1.20. 3-Nitro-**13b**-(trifluoromethyl)-**13b**,l4-dihydrorutaecarpine (**11**)*

A mixture of 3-(2-(1H-indol-3-yl)ethyl)-6-nitro-2-(trifluoromethyl)quinazolin-4(3H)-one **10** (8.0 g), acetic acid (40 mL) and hydrochloric acid (6 mL) was heated under reflux for 1 h. After the reaction mixture was cooled, it was diluted with water (50 mL) and the precipitate formed was filtered off, washed with water. The solid obtained was dried under vacuum to give yellow-green powder (**8**). m.p. 266–269 °C; ^{1}H NMR (400 MHz, DMSO-d_6): δ 10.97 (s, 1H), 9.12 (s, 1H), 8.56 (d, 1H, J = 2.7), 8.26 (dd, 1H, J = 9.0, 2.7), 7.59 (dd, 1H, J = 11.4, 8.1), 7.27 (m, 1H), 7.10 (m, 2H), 2.98(m, 2H), 2.84 (m, 2H); ESI-MS m/z: 401 $[M - H]^-$.

*5.1.21. 3-Amino-**13b**-(trifluoromethyl)-**13b**,l4-dihydro-rutaecarpine (**12**)*

3-Nitro-**13b**-(trifluoromethyl)-**13b**,l4-dihydrorutaecarpine **11** (4.0 g) was hydrogenated in a solution of MeOH (300 mL) at 40–45 lb/inch^2 of H_2 using 10% Pd/C (1.2 g) as catalyst for 8 h. The catalyst was filtered off, and the filtrate was evaporated under reduced pressure to give an brown solid (80%). m.p. 177–179 °C; ^{1}H NMR (400 MHz, DMSO-d_6): δ 11.11 (s, 1H), 7.95 (s, 1H), 7.57 (d, 1H, J = 7.8), 7.50 (d, 1H, J = 8.2), 7.20 (m, 2H), 7.09 (m, 2H), 6.79(s, 1H), 6.71(m, 1H), 6.63(d,1H, J = 8.4), 2.89(s, 2H), 2.84 (m, 2H); ESI-MS m/z: 373 $[M + H]^+$.

*5.1.22. N-(2-(1H-Indol-3-yl)ethyl)-2-amino-5-nitrobenzamide (**13**)*

A mixture of tryptamine (3.2 g) and 6-nitro-1H-benzo[d][1,3]oxazine-2,4-dione **9** (5.2 g) was refluxed in ethanol (20 mL) for 1 h. After cooling the crystals formed were collected and dried to afford a light yellow solid (67%). m.p. 181–182 °C; ^{1}H NMR (400 MHz, DMSO-d_6): δ 10.83(s, 1H), 8.85 (s, 1H), 8.49(d, 1H, J = 2.6), 8.02 (dd, 1H, J = 9.2, 2.6), 7.79 (s, 2H), 7.59(d, 1H, J = 7.8), 7.34(d, 1H, J = 8.1), 7.18(d, 1H, J = 2.1), 7.07(t, 1H, J = 7.8), 6.98(t, 1H, J = 7.4), 6.80(d, 1H, J = 9.2), 3.51(dd, 2H, J = 13.5, 7.0), 2.96(t, 2H, J = 7.4); ESI-MS m/z: 325 $[M + H]^+$.

*5.1.23. N-(2-(1H-Indol-3-yl)ethyl)-2,5-diaminobenzamide (**14**)*

N-(2-(1H-Indol-3-yl)ethyl)-2-amino-5-nitrobenzamide **13** (2.9 g) in a solution of MeOH (300 mL) at 40–45 lb/inch^2 of H_2 using 10% Pd/C (1.0 g) as catalyst for 8 h. The catalyst was filtered off, and the filtrate was evaporated under reduced pressure to give an gray solid (87%). m.p. 178–179 °C; ^{1}H NMR (400 MHz, DMSO-d_6): δ 10.80 (s, 1H), 8.19 (t, 1H, J = 5.6), 7.58 (d, 1H, J = 7.8), 7.34 (d, 1H, J = 8.0), 7.17 (d, 1H, J = 2.1), 7.07 (m, 1H), 6.99 (t, 1H, J = 7.0), 6.71(d, 1H, J = 2.4), 6.55(dd,1H, J = 8.5, 2.5), 6.49(d, 1H, J = 8.5), 5.39(s, 2H), 4.33(s, 2H), 3.46(d, 2H, J = 8.1), 2.84 (m, 2H); ESI-MS m/z: 373 $[M + H]^+$.

5.2. Biological activity and molecular modeling

5.2.1. In vitro inhibition studies on AChE and BuChE

Acetylcholinesterase (AChE, E.C. 3.1.1.7, from *electric eel*), butylcholinesterase (BuChE, E.C. 3.1.1.8, from *equine serum*), 5,5′-dithiobis-(2-nitrobenzoic acid) (Ellman's reagent, DTNB), butylthiocholine chloride (BTC), acetylthiocholine chloride (ATC), and tarcine hydrochloride were purchased from SigmaeAldrich.

In vitro AChE assay: All the assays were under 0.1 M KH_2PO_4/K_2HPO_4 buffer, pH 8.0, using a Shimadzu 2450 Spectrophotometer. Enzyme solutions were prepared to give 2.0 units/mL in 2 mL aliquots. The assay medium contained phosphate buffer, pH 8.0 (1 mL), 50 μl of 0.01 M DTNB, 10 μL of enzyme, and 50 μL of 0.01 M substrate (Acetylthiocholine chloride). The substrate was added to the assay medium containing enzyme, buffer, and DTNB with inhibitor after 15 min of incubation time. The activity was determined by measuring the increase in absorbance at 412 nm at 1 min intervals at 37 °C. Calculations were performed according to the method of the equation in Ellman [19] et al. *In vitro* BuChE assay use the similar method described above.

To determine the time-dependence of AChE inhibition, AChE was incubated in the presence of **5c** at 25 °C, and the residual activity was determined at various time intervals (from 15 to 75 min). The enzyme (0.6 unit) was incubated with 5 nM of **5c** in phosphate buffer of a total volume of 500 μL. After 30 min incubation at 25 °C, the mixture was chilled in an ice bath. The samples were dialyzed in phosphate buffer at 4 °C, and the residual activity was recorded after various dialysis time. The residual enzyme activity was determined before and after dialysis. A control experiment was performed under identical conditions without inhibitor. The AChE inhibitory activity was assayed using the method of Ellman.

Kinetic characterization of AChE and BuChE was performed using a reported method. Six different concentrations of substrate were mixed in the 1 mL 0.1 M KH_2PO_4/K_2HPO_4 buffer (pH 8.0), containing 50 μL of DTNB, 10 μL AChE, and 50 μL substrate. Test compound was added into the assay solution and pre-incubated with the enzyme at 37 °C for 15 min, followed by the addition of

substrate. Kinetic characterization of the hydrolysis of ATC catalyzed by AChE was done spectrometrically at 412 nm. A parallel control with no inhibitor in the mixture, allowed adjusting activities to be measured at various times. Kinetic characterization of BuChE assay use the similar method described above.

5.2.2. Molecular modeling

The crystal structure of acetylcholinesterase complexed with E2020 (code ID:1EVE) and the Human Butyrylcholinesterase complexed with Echothiophate (code ID: 1POI) were obtained in the Protein Data Bank after eliminating the inhibitor (E2020) and water molecules. The 3D Structure of **5c** was built and performed geometry optimization by molecular mechanics. Further preparation of substrates included addition of Gasteiger charges, removal of hydrogen atoms and addition of their atomic charges to skeleton atoms, and finally, assignment of proper atomic types. Autotors was then used to define the rotatable bonds in the ligands.

Docking studies were carried out using the AUTODOCK 4.0 program. Using ADT, Polar hydrogen atoms were added to amino acid residues and Gasteiger charges were assigned to all atoms of the enzyme. The resulting enzyme structure was used as an input for the AUTOGRID program.

AUTOGRID performed a precalculated atomic affinity grid maps for each atom type in the ligand plus an electrostatics map and a separate desolvation map present in the substrate molecule. All maps were calculated with 0.375 Å spacing between grid points. The centre of the grid box was placed at the bottom of the active site gorge (AChE [2.781 64.383 67.971]; BuChE [112.0 20.0 40.0]). The dimensions of the active site box were set at 50 $\times$ 46 $\times$ 46 Å.

Flexible ligand docking was performed for the compounds. Docking calculations were carried out using the Lamarckian genetic algorithm (LGA) and all parameters were the same for each docking. We used initially a population of random individuals (population size: 150), a maximum number of 2,500,000 energy evaluations, a maximum number of generations of 27,000, At the end of a docking procedure (100 docking runs), the resulting positions were clustered according to a root mean square criterion of 0.5 Å.

Acknowledgment

We thank the National Nature Science Foundation of China (20772159, 90813011, U0832005), the NSFC/RGC joint Research Scheme (30731160006) for financial support of this study.

References

[1] P. Davies, A.J.F. Maloney, Lancet 2 (1976) 1403.
[2] R.T. Bartus, R.L. Dean III, B. Beer, A.S. Lippa, Science 217 (1982) 408–414.
[3] M.J. assoulié, F. Bacou, E. Barnard, A. Chatonnet, B.P. Doctor, D.M. Quinn (Eds.), Cholinesterases: Structure, Function, Mechanism, Genetics and Cell Biology, American Chemical Society, Washington, 1991.
[4] J. Hardy, D.J. Selkoe, Science 297 (2002) 353–356.
[5] G.V. De Ferrari, M.A. Canales, I. Shin, L.M. Weiner, I. Silman, N.C. Inestrosa, Biochemistry 40 (2001) 10447–10457.
[6] M.M. Mesulam, M. Asuncion Moran, Ann. Neurol. 22 (1987) 223–228.
[7] M. Weinstock, CNS Drugs 12 (1999) 307–323.
[8] G. Pacheco, R. Palacios-Esquivel, D.E. Moss, J. Pharmacol. Exp. Ther. 274 (1995) 767–770.
[9] D.R. Liston, J.A. Nielsen, A. Villalobos, D. Chapin, S.B. Jones, S.T. Hubbard, A. Shalaby, A. Ramirez, D. Nason, W.F. White, Eur. J. Pharmacol. 486 (2004) 9–17.
[10] D.E. Kuhl, R.A. Koeppe, S.E. Snyder, S. Minoshima, K.A. Frey, M.R. Kilbourn, Ann. Neurol. 59 (2006) 13–20.
[11] E.H. Rydberg, B. Brumshtein, H.M. Greenblatt, D.M. Wong, D. Shaya, L.D. Williams, et al., J. Med. Chem. 49 (2006) 5491–5500.
[12] N. Akula, L. Lecanu, J. Greeson, V. Papadopoulos, Bioorg. Med. Chem. Lett. 16 (2006) 6277–6280.
[13] G. Kryger, I. Silman, J.L. Sussman, Structure 7 (1999) 297–307.
[14] T.H. Tsai, T.F. Lee, C.F. Chen, L.C.H. Wang, Pharmacol. Biochem. Behav. 50 (1995) 293–298.
[15] J.R. Sheu, Cardiovasc. Drug Rev. 17 (1999) 237–298.
[16] T.C. Moon, M. Murakami, I. Kudo, K.H. Son, H.P. Kim, S.S. Kang, H.W. Chang, Inflamm. Res. 48 (1999) 621–625.
[17] C.H. Park, S.H. Kim, W. Choi, Y.L. Lee, J.S. Kim, S.S. Kang, Y.H. Suh, Planta Med. 62 (1996) 405–409.
[18] M. Decker, Eur. J. Med. Chem. 40 (2005) 305–313.
[19] G.L. Ellman, K.D. Courtney, V. Andres Jr., R.M. Featherstone, Biochem. Pharmacol. 7 (1961) 88–95.
[20] J. Bergman, S. Bergman, J. Org. Chem. 50 (1985) 1246–1255.
[21] H. Tang, Y.-B. Wei, C. Zhang, F.-X. Ning, W. Qiao, S.-L. Huang, L. Ma, Z.-S. Huang, L.-Q. Gu, Eur. J. Med. Chem. 44 (2009) 2523–2532.
[22] H. Tang, F.-X. Ning, Y.-B. Wei, S.-L. Huang, Z.-S. Huang, A.S.-C. Chan, L.-Q. Gu, Bioorg. Med. Chem. Lett. 17 (2007) 3765–3768.
[23] G.M. Morris, D.S. Goodsell, R.S. Halliday, R. Huey, W.E. Hart, R.K. Belew, A.J. Olson, J. Comput. Chem. 19 (1998) 1639–1662.
[24] W.L. DeLano, The PyMOL Molecular Graphics System. DeLano Scientific. San Carlos, CA.
[25] J. Das, M.S. Kumar, D. Subrahmanyam, T.V.R.S. Sastry, et al., Bioorg. Med. Chem. 14 (2006) 8032–8042.